Biochemical and Biophysical Research Communications 426 (2012) 601–607

Contents lists available at SciVerse ScienceDirect

Biochemical and Biophysical Research Communications

journal homepage: www.elsevier.com/locate/ybbrc

Modeling the Zn^{2+} and Cd^{2+} metalation mechanism in mammalian metallothionein 1a

Duncan E.K. Sutherland [a], Kelly L. Summers [b], Martin J. Stillman [a,b,*]

[a] Department of Biology, The University of Western Ontario, London, Ontario, Canada N6A 5B7
[b] Department of Chemistry, The University of Western Ontario, London, Ontario, Canada N6A 5B7

ARTICLE INFO

Article history:
Received 21 August 2012
Available online 6 September 2012

Keywords:
Human metallothionein
Metal-binding domains
Cooperative metalation
Noncooperative metalation
Cadmium and zinc binding
Mechanism of metalation

ABSTRACT

Mammalian metallothioneins (MTs) are a family of small cysteine rich proteins believed to have a number of physiological functions, including both metal ion homeostasis and toxic metal detoxification. Mammalian MTs bind 7 Zn^{2+} or Cd^{2+} ions into two distinct domains: an N-terminal β-domain that binds 3 Zn^{2+} or Cd^{2+}, and a C-terminal α-domain that binds 4 Zn^{2+} or Cd^{2+}. Although stepwise metalation to the saturated M_7-MT (where M = Zn^{2+} or Cd^{2+}) species would be expected to take place via a noncooperative mechanism involving the 20 cysteine thiolate ligands, literature reports suggest a cooperative mechanism involving cluster formation prior to saturation of the protein. Electrospray ionization mass spectrometry (ESI-MS) provides this sensitivity through delineation of all species (M_n-MT, $n = 0–7$) coexisting at each step in the metalation process. We report modeled ESI-mass spectral data for the stepwise metalation of human recombinant MT 1a (rhMT) and its two isolated fractions for three mechanistic conditions: cooperative (where the binding affinities are: $K_1 < K_2 < K_3 < \cdots < K_7$), weakly cooperative (where $K_1 = K_2 = K_3 = \cdots = K_7$), and noncooperative, (where $K_1 > K_2 > K_3 > \cdots > K_7$). Detailed ESI-MS metalation data of human recombinant MT 1a by Zn^{2+} and Cd^{2+} are also reported. Comparison of the experimental data with the predicted mass spectral data provides conclusive evidence that metalation occurs in a noncooperative fashion for Zn^{2+} and Cd^{2+} binding to rhMT 1a.

1. Introduction

Metallothioneins (MTs) are a ubiquitous group of metalloproteins characterized by their small size, high cysteine content, lack of aromatic amino acids, and their ability to bind a wide range of metal ions [1]. Mammalian MTs are the most well studied members of the MT family and consist of 20 cysteine residues that act to encapsulate two metal-thiolate cores. Fig. 1A shows a space filling model of recombinant human MT 1a coordinated to 7 Cd^{2+} ions (Cd_7-βα-rhMT 1a; mammalian isoforms other than 1a will be noted specifically). The sequence of the cleaved recombinant βα-rhMT coordinated to seven divalent metal ions is shown in Fig. 1C, with the metal ions colored green and cysteine residues yellow. The numbering of the cadmium-thiolate core is cross referenced to the original naming conventions based on the order of the NMR bands in the mammalian Cd_7-MT 2a spectra [2], while the numbering of the cysteine residues has been adjusted to accommodate both the additional amino acids from thrombin cleavage (residues 1 and 2) and a series of amino acids meant to aid in protein expression (residues 3–9). The connectivity for metal-S_{CYS} bonding is shown for the 7 metal species. Note the presence of bridging cys that connect the divalent metals together in metal-thiolate clusters. Because these soft, divalent, Group 10 metals bind to thiolates with tetrahedral coordination, the maximum number of metals bound without using bridging cys would be 5 $(MS_4)^{2-}$. Indeed for As^{3+} the maximum is found without bridges forming: $As_6Scys_{18}H_2$-rhMT [3]. Bridging increases the maximum number of divalent metals that can bind [4].

When metal-saturated, MT binds using two independent domains: an N-terminal β-domain and a C-terminal α-domain [5,6]. The β-domain is capable of binding 3 Zn^{2+} or Cd^{2+} ions through 9 cysteine residues, while the α-domain is capable of binding 4 Zn^{2+} or Cd^{2+} ions through 11 cysteine residues (Fig. 1B). Structural data have only been reported from metal-saturated proteins, leaving the exact mechanism of metalation under debate. It is important to note that while Zn^{2+} and Cd^{2+} bind to metallothionein in an isostructural manner and the overall molecular architecture of the protein when coordinated to Zn^{2+} or Cd^{2+} is identical, their binding affinities differ by a factor of 10^3 [4,7].

MT has been implicated in a range of functions, including metal ion homeostasis, toxic metal detoxification, and as a protective agent against oxidative stress [4,7]. Each of these proposed

* Corresponding author at: Department of Chemistry, The University of Western Ontario, London, Ontario, Canada N6A 5B7.
E-mail address: martin.stillman@uwo.ca (M.J. Stillman).

0006-291X/$ - see front matter © 2012 Elsevier Inc. All rights reserved.
http://dx.doi.org/10.1016/j.bbrc.2012.08.136

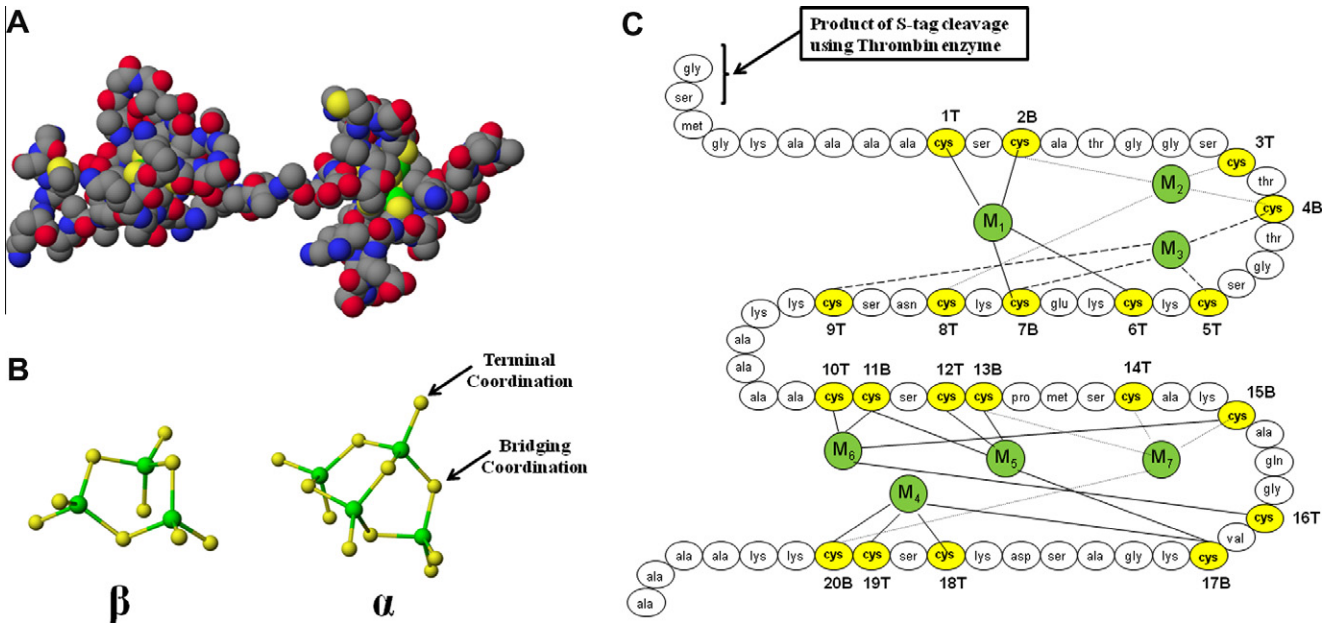

Fig. 1. (A) Space filling structure of cadmium-metallated recombinant human MT 1a (Cd_7-βα-rhMT 1a) calculated using molecular modeling. The N-terminal β-domain is located on the left hand side, while the C-terminal α-domain is located on the right-hand side. (B) The cadmium-cysteinyl-thiolate connections, both terminal and bridging, in Cd_7-βα-rhMT 1a are presented as a ball-and-stick model: β-domain (left) and α-domain (right). The α-domain has one bridging and one terminal thiolate labeled to clearly illustrate the different modes of coordination. (C) Connectivity diagram of human metallothionein 1a, which shows that each of the 7 Cd^{2+} are connected to exactly 4 cysteines in a tetrahedral arrangement. The cysteine residues have been numbered 1–20 and with the additional label T or B representing terminal or bridging cysteine thiolates, respectively. In the nomenclature used here, the 'recombinant' source is noted by a prefix of 'r', and the origin of the sequence is indicated by the second prefix, here 'h' for human. Molecular modeling data from Chan et al. [17].

functions relies upon the mechanism of metalation, because it is this mechanism that will determine the available metalation states of the protein.

The mechanism for the stepwise metalation of a protein with multiple binding sites would be expected to be noncooperative, meaning that each metal binds unaffected by the previous metals if the binding sites were not themselves related to one another. Under these conditions, the binding affinities of the metals will decrease statistically as the binding sites fill (resulting in $K_1 > K_2 > K_3 > \cdots > K_7$). This has been shown in kinetic analysis in which 6 As^{3+} bound rhMT 1a [3]. However, in the case of Cd^{2+} and Zn^{2+} the ability to form bridged-clusters (Fig. 1) when the protein is saturated with 7 metals has added a layer of complexity to metalation studies.

Over many years studies have supported a cooperative mechanism [8,9], where the binding of one metal facilitates the binding of the next metal (resulting in $K_1 < K_2 < K_3 < \cdots < K_7$). A cooperative mechanism, where the binding of one metal ion facilitates further binding, would push towards the species with the greatest *K*, for example the fully metalated MT and the metal free, apoMT would be the only components. If, however, the mechanism of metalation is noncooperative, where metalation events follow a statistically declining set of binding affinities (*K*s), then during a titration partially metalated intermediates would be present equally before formation of the fully metalated species. Apo-MT would be consumed according to the values of the *K*s and the stoichiometric ratio of metal added at any time.

A number of electrospray ionization mass spectrometry (ESI-MS) studies have suggested that the mechanism of metalation is in fact noncooperative [3,10–16]. While the majority of these studies have been carried out on mammalian MT, a single study of seaweed MT suggests that this mechanism may be more general.

To date there have been no reports of the predicted pattern from ESI-MS data in terms of the binding mechanism. The exact distribution of metalated species (M_n-MT, $n = 0–7$) can be calculated based on the ratios of the K_ns ($n = 1–7$). From a detailed examination of ESI-MS data, we have formulated models for three metalation mechanisms and calculated the mass spectral data patterns expected during titrations of MT with divalent metals. These models provide the necessary data to unambiguously establish the metal ion speciation that will be present for cooperative, weakly cooperative and noncooperative metalation. By comparing the experimental ESI-MS data during metalation of MT with these predicted data, we have determined that rhMT 1a metalates in a noncooperative manner. This paper provides a framework for analyzing and interpreting ESI-mass spectral data in mechanistic terms so that in future the pattern of metallated species is clearly stated.

2. Materials and methods

2.1. Chemicals

$CdSO_4$ (J.T. Baker Chemical Company). Chemicals used in this study were of the highest-grade purity from commercial sources. Solutions were made with >14 MΩ cm^{-1} deionized water (Barnstead Nanopure Infinity). Protein purification steps were performed on Hi Trap SP ion exchange columns, fine G-25 Sephadex (Amersham Biosciences) and a stirred ultrafiltration cell (Amicon Bioseparations/Millipore) with a YM-3 membrane (3000 MWCO).

2.2. Protein preparation

The expression and purification methods used to purify human recombinant MT isoform 1a have been previously reported [17]. β-rhMT, α-rhMT and βα-rhMT 1a proteins have 38-residue, 41-residue, and 72-residue sequences, respectively: β-rhMT MGKAAA-ACSC ATGGSCTCTG SCKCKECKCN SCKKAAAA, α-rhMT MGKAAAAC CSCCPMSCAK CAQGCVCKGA SEKCSCCKKA AAA, βα-rhMT

MGKAAAACSC ATGGSCTCTG SCKCKECKCN SCKKAAAACC SCCPMSCAKC AQGCVCKGAS EKCSCCKKAA AA. There are 9, 11, and 20 cysteine residues present in β-rhMT, α-rhMT and βα-rhMT, respectively, and no disulfide bonds. The presence of the extra tetra-alanine sequence in this recombinant construct has not resulted in data different from that previously reported by ^{113}Cd NMR [2,18]. The expression system included, for stability purposes, an N-terminal S-tag (MKETAAAKFE RQHMDSPDLG TLVPRGS). Recombinant proteins were expressed in BL21(DE3) *Escherichia coli*. All cell lines were transformed using the pET29a plasmid. Removal of the S-tag was performed using a Thrombin CleanCleave™ Kit (Sigma). All protein samples were argon saturated and rigorously evacuated. Concentrated HCl was used to demetalate protein samples, followed by desalting on G-25 (Sephadex). Unless specifically stated otherwise, all data discussed in this paper are from recombinant, human MT isoform 1a with the specific sequence shown above.

2.3. ESI-MS procedures

Protein concentrations were determined by remetalation of a portion of the sample with Cd^{2+} ions; and the Cd–MT formed was monitored by UV absorption spectroscopy using the absorbance at 250 nm ($\varepsilon_{\beta 250}$ = 36,000 M^{-1} cm^{-1}; $\varepsilon_{\alpha 250}$ = 45,000 M^{-1} cm^{-1}; $\varepsilon_{\beta\alpha 250}$ = 89,000 M^{-1} cm^{-1}). Zinc sulfate, cadmium sulfate, and all molar equivalents were calibrated using atomic absorption spectrometry.

Data were collected on an electrospray-ionization time-of-flight (ESI-TOF) mass spectrometer (Bruker Daltonics) in the positive ion mode. NaI was used as the calibrant. The scan conditions for the spectrometer were: end plate offset, −500 V; capillary, +4200 V; nebulizer, 2.0 bar; dry gas flow, 8.0 L/min; dry temperature, 80 °C; capillary exit, 180 V; skimmer 1, 22.0 V; hexapole 1, 22.5 V; hexapole RF, 600 Vpp; skimmer 2, 22 V; lens 1 transfer, 88 μs; lens 1 pre pulse storage, 23 μs. The range was 500.0–3000.0 *m*/*z*, averaging 2 × 0.5 Hz. Spectra were deconvoluted using the Bruker Compass DataAnalysis software package. There is almost no change in the ESI-MS spectra over the range pH (6–9).

2.4. Mechanistic modeling

Simulated mechanistic data were based on the sequential, bimolecular metalation of MT with the distribution of metalated species being directly related to the product of both the amount of starting material, and the association constant (K_N).

3. Results

The stepwise metalation equations for the metal free, isolated fragments (H_{11}-α-rhMT 1a; H_9-β-rhMT 1a) and the full protein (H_{20}-βα-rhMT 1a) by Zn^{2+} are shown below:

$$\mathrm{Apo\alpha hMT} + \mathrm{Zn^{2+}} \xrightarrow{K_{1\alpha}} \mathrm{Zn_1 - H_9 - \alpha hMT}$$

$$\mathrm{Zn_1\alpha hMT} + \mathrm{Zn^{2+}} \xrightarrow{K_{2\alpha}} \mathrm{Zn_2 - H_7 - \alpha hMT}$$

$$\mathrm{Zn_2\alpha hMT} + \mathrm{Zn^{2+}} \xrightarrow{K_{3\alpha}} \mathrm{Zn_3 - H_5 - \alpha hMT}$$

$$\mathrm{Zn_3\alpha hMT} + \mathrm{Zn^{2+}} \xrightarrow{K_{4\alpha}} \mathrm{Zn_4 - H_3 - \alpha hMT}$$

$$\mathrm{Apo\beta hMT} + \mathrm{Zn^{2+}} \xrightarrow{K_{1\beta}} \mathrm{Zn_1 - H_7 - \beta hMT}$$

$$\mathrm{Zn_1\beta hMT} + \mathrm{Zn^{2+}} \xrightarrow{K_{2\beta}} \mathrm{Zn_2 - H_5 - \beta hMT}$$

$$\mathrm{Zn_2\beta hMT} + \mathrm{Zn^{2+}} \xrightarrow{K_{3\beta}} \mathrm{Zn_3 - H_3 - \beta hMT}$$

$$\mathrm{Apo\beta\alpha hMT} + \mathrm{Zn^{2+}} \xrightarrow{K_{1\beta\alpha}} \mathrm{Zn_1 - H_{18} - \beta\alpha hMT}$$

$$\mathrm{Zn_1\beta\alpha hMT} + \mathrm{Zn^{2+}} \xrightarrow{K_{2\beta\alpha}} \mathrm{Zn_2 - H_{16} - \beta\alpha hMT}$$

$$\mathrm{Zn_2\beta\alpha hMT} + \mathrm{Zn^{2+}} \xrightarrow{K_{3\beta\alpha}} \mathrm{Zn_3 - H_{14} - \beta\alpha hMT}$$

$$\mathrm{Zn_3\beta\alpha hMT} + \mathrm{Zn^{2+}} \xrightarrow{K_{4\beta\alpha}} \mathrm{Zn_4 - H_{12} - \beta\alpha hMT}$$

$$\mathrm{Zn_4\beta\alpha hMT} + \mathrm{Zn^{2+}} \xrightarrow{K_{5\beta\alpha}} \mathrm{Zn_5 - H_{10} - \beta\alpha hMT}$$

$$\mathrm{Zn_5\beta\alpha hMT} + \mathrm{Zn^{2+}} \xrightarrow{K_{6\beta\alpha}} \mathrm{Zn_6 - H_8 - \beta\alpha hMT}$$

$$\mathrm{Zn_6\beta\alpha hMT} + \mathrm{Zn^{2+}} \xrightarrow{K_{7\beta\alpha}} \mathrm{Zn_7 - H_6 - \beta\alpha hMT}$$

This set of chemical equations represents the complete metalation of each protein where the binding affinities are represented by an equilibrium constant K (n = (α) 1–4; (β) 1–3; (βα) 1–7). When the values of K are very high (here of the order 10^{10}), then although the complete system is in equilibrium, addition of stoichiometric quantities of protein and zinc will lead to formation of the final product in almost quantitative yield. Under these conditions addition of aliquots of Zn^{2+} or Cd^{2+} will result in a product that balances the exact speciation based on the relative values of each set of *K*s for the whole reaction.

In Fig. 2 we report the speciation at each of several steps in the experimental ESI-MS data for a titration of Cd^{2+} into apo-β-rHMT, apo-α-rHMT, and apo-βα-rHMT, respectively. The bar graphs (B, D and F) clearly show the presence of multiple species for each equivalent of Cd^{2+} added. The metalation status for each protein can readily be plotted in bar graph form because whole numbers of metals are bound. Considering the metalation of the full, βα-rhMT (E and F) we find that for each step in the metalation titration, the dominant species formed only represents about 40% of the total speciation. The other species (flanking the dominant form) represent over 50% of the metal added at that point. There is no indication of the formation of a dominant species with more than 60% of the metal added until 7 Cd^{2+} have been added. Very similar metalation properties have been reported recently for the Zn^{2+} metalation of these same protein species [19]. The contour plots show conclusively that the number of metals bound to MT, and its isolated domains, is directly related to the number of metals added to solution. The linearity in the metalation supports a noncooperative mechanism as we will show below in Fig. 3.

As described above, the calculated models of the experimental data provide unambiguous indicators of the mechanism because the fraction of each of the partially metalated proteins is shown in the experimental ESI-MS data. We should note that many spectroscopic techniques, such as CD and UV absorption spectroscopy, measure the average metalation state and are not sensitive to the specific metalated states of MT.

Fig. 3 compares the experimental data for Cd^{2+} (A–C) and Zn^{2+} (D–F) metalation of the rhMT protein with predicted speciation based on three mechanistic models. The theoretical metalation curves for a noncooperative system (where $K_1 > K_2 > K_3 > \cdots > K_n$; G–I), a weakly cooperative system, (where $K_1 = K_2 = K_3 = \cdots = K_n$; J–L), and a strongly cooperative system (where $K_1 < K_2 < K_3 < \cdots < K_n$; M–O). The speciation predicted is color coded to match the speciation in the experimental ESI-MS data. For a noncooperative mechanism, the distribution of metals represents a declining value in *K*, so that the final product only appears following the formation of the intermediate species. Consequently, the maxima of

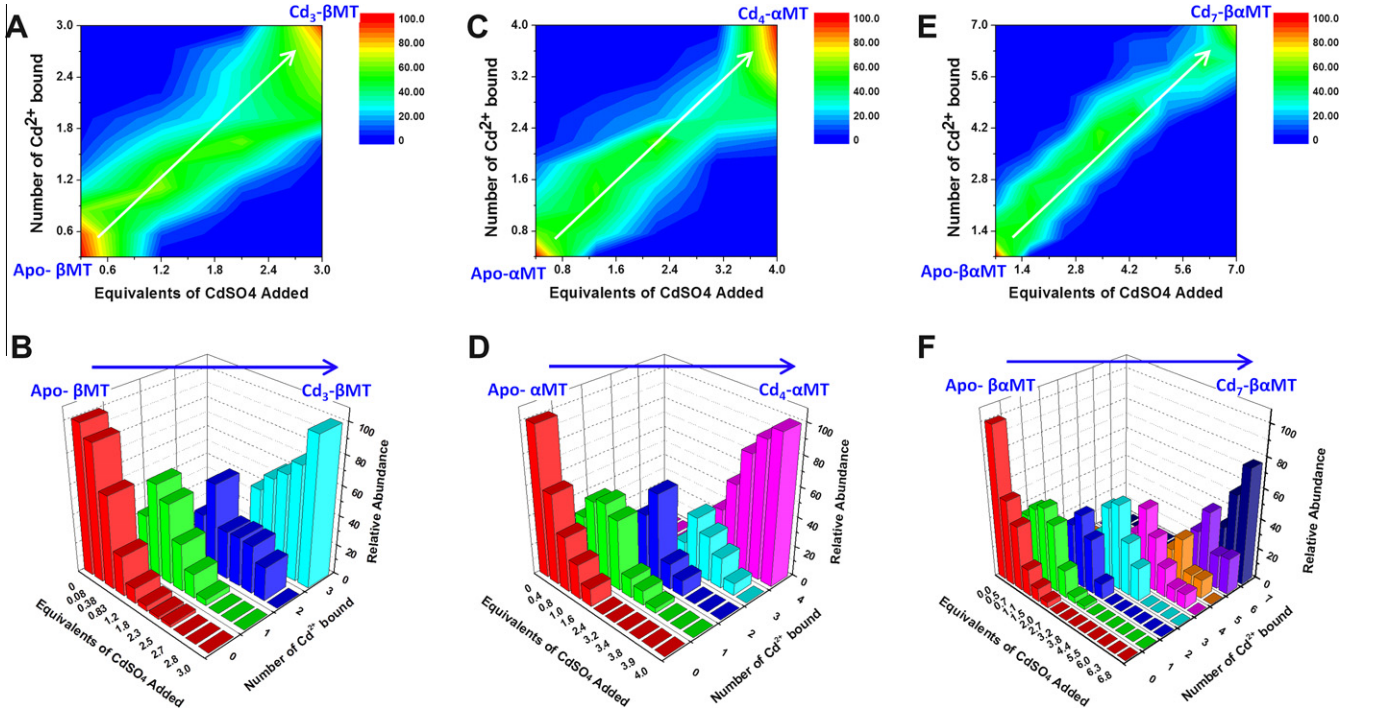

Fig. 2. Experimental ESI-MS data for the stepwise metalation represented as contours (A, C, E) and bar graphs (B, D, F) for β-, α-, and βα-rhMT 1a as a function of Cd^{2+} added. (A, C, E) A top-down view of metalation, showing the linear progression from apo- to fully metalated peptide as a function of Cd^{2+} added to solution. The adjacent legend ranges between 100% abundance (red) and 0% abundance (dark blue). (B, D, F) A side-on view of metalation, which shows the relative abundance of each species as a function of Cd^{2+} added to solution. Color code: metal free is red; Cd_1 is green; Cd_2 is dark blue; Cd_3 is light blue; Cd_4 is light purple; Cd_5 is orange; Cd_6 is violet; Cd_7 is indigo. In both sets of graphs, as the total amount of Cd^{2+} added to the solution is increased, the number of metals bound to the peptides also increases. These graphs include deconvoluted mass spectral data previously reported by Rigby-Duncan et al. [20], and Sutherland et al. [10,19]. (For interpretation of the references to colour in this figure legend, the reader is referred to the web version of this article.)

each metalation state should be roughly equal as the metalation proceeds through the series of biomolecular reactions. For a weakly cooperative mechanism (J–L), we immediately see that the maximum intensity of all the intermediate species, except M_1-MT (where M = either Cd^{2+} or Zn^{2+}), is suppressed leading to the early formation of fully metalated MT, as well as the persistence of the metal free protein. This trend is further enhanced in the strongly cooperative mechanism of metalation (M-O), where the early formation of the fully metalated MT is observed.

The predicted mass spectral data for a cooperative mechanism is dramatically different than that predicted for a noncooperative mechanism because the final K is greater than all previous *K* values and so forces formation of the product using the metal bound in partially metalated species.

The models in Fig. 3 show that if these proteins were metalated in a cooperative manner, the appearance of fully metalated MT would be expected in the experimental data at the 1-metal-added point and the partially metalated species would be very weak or almost nonexistent for all added equivalents. Further, only the metal free and fully metalated forms of the protein would dominate. Comparison between the experimental data and the modeled data in Fig. 3 provides strong evidence that metalation occurs via a noncooperative mechanism.

A final data set can be calculated that shows the actual distribution of metalated species. These spectral traces are easier to compare directly with experimental ESI-MS data. In Fig. 4, we show the experimental data in (A) and the simulated deconvoluted mass spectra in (B, C and D) for two additions (0.9 and 5.9 equivalents) of Zn^{2+} to the full protein based on the three mechanistic models. The two points chosen provide a clear differentiation between the three possible mechanisms. In the noncooperative mechanism (B), the dominant species is related to the number of equivalents of Zn^{2+} added to the solution, so that consequently at 0.9 eq. of Zn^{2+} Zn_1-βα-rhMT is dominant, but at 5.9 eq. of Zn^{2+} Zn_6-βα-rhMT is dominant. The weakly cooperative mechanism (C) demonstrates an initial metalation pattern similar to that of the noncooperative mechanism; however at greater equivalents the fully metalated form is favored. As expected, the cooperative mechanism requires that the dominant forms of metalation be either the fully metalated or the metal free forms (prior to the addition of sufficient metal) with very low concentrations of partially metalated intermediates present.

From Figs. 3 and 4, it is clear that the mechanism of metalation of rhMT 1a with Zn^{2+} and Cd^{2+} is noncooperative. The model data demonstrate that there are significant differences in the metalation pattern of a cooperative and a noncooperative mechanism and that ESI-MS data are sensitive to these differences.

4. Discussion

Our understanding of the detailed functional dependence of MT as a metallochaperone relies greatly on our understanding of its metalation properties. Unfortunately, these metalation properties also make the mechanistic study of MT difficult; specifically (1) a similar coordination environment for all bound metal ions; (2) the high affinity of the cysteinyl-thiolates of MT for divalent metal ions (Zn^{2+} and Cd^{2+}); and (3) the lack of a spectroscopic probe that can readily discriminate between the differently metalated states of MT.

As a result, the mechanism of metalation of mammalian MT has been intensively debated with different reports suggesting either a cooperative or noncooperative mechanism of metalation. Recent ESI-MS data have provided significant new information about the early stages of metalation of metalloproteins, as well as the discovery of the supermetalated (metalation in excess of traditional lev-

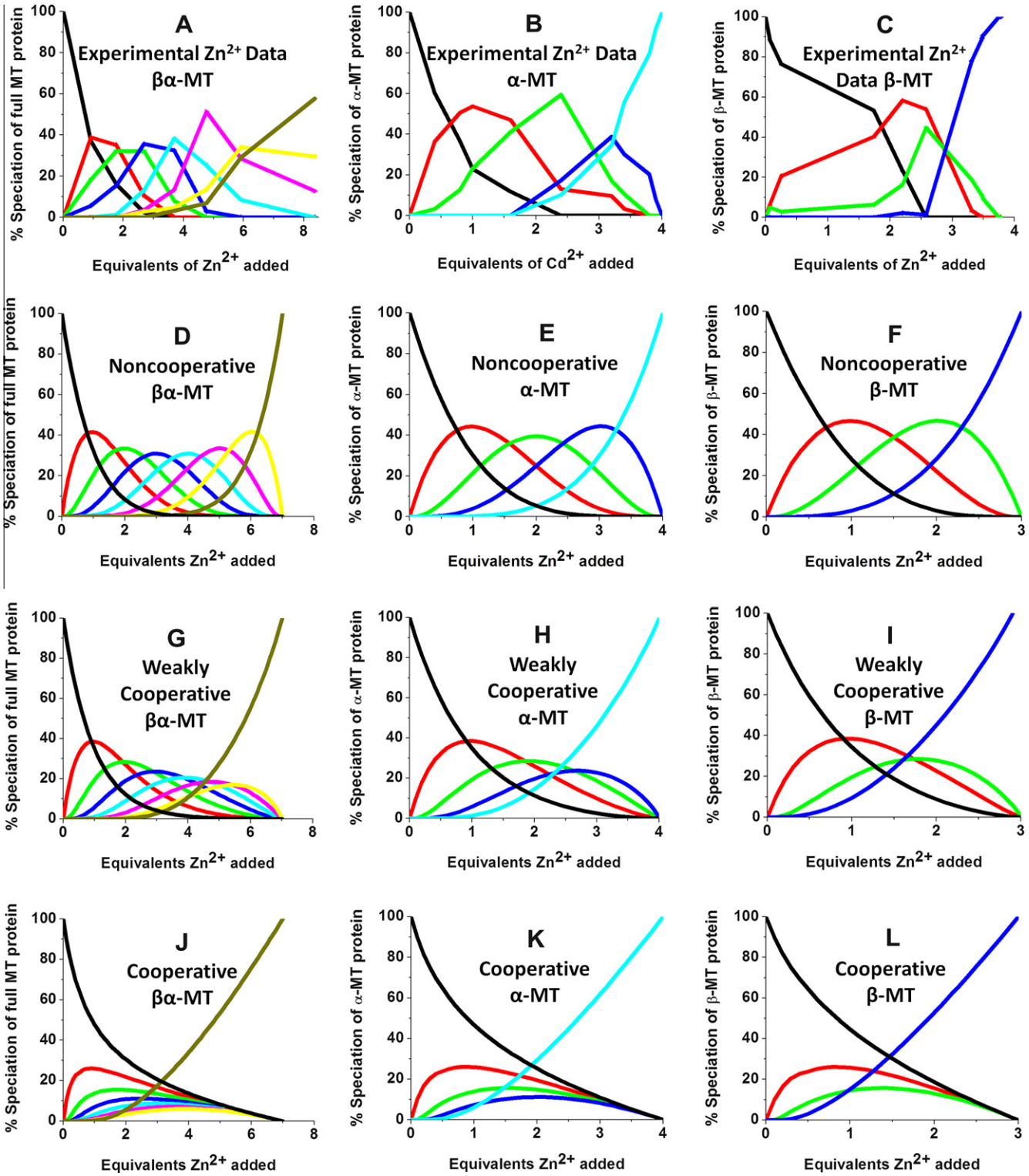

Fig. 3. Experimental and theoretical data showing Cd^{2+} (A, B, C) and Zn^{2+} (D, E, F) speciation during metalation of the full MT protein, as well as the α- and β-domains. Modeled data: (G, H, I) A model using noncooperativity rules (declining K_as) of ESI-MS data. (J, K, L) A model using weakly cooperativity rules (equal K_as). (M, N, O) A model using strongly cooperativity rules (increasing K_as). Each line corresponds to a different metalation state: Zn_0 (—●—), Zn_1 (-■-), Zn_2 (-▲-), Zn_3 (-▼-), Zn_4 (-◆-), Zn_5 (-★-), Zn_6 (-◀-) and Zn_7 (-▶-).

els) forms of MT [11,18,20–22]. These data were previously considered difficult (if not impossible) to obtain by other methods [23,24].

In addition to confusion regarding the mechanism, there has also been uncertainty in the exact species formed following the addition of sub-saturating numbers of metal ions. Prior to reports of metalation titrations using ESI-MS, MT was often assumed to be homogenously metalated, meaning that the addition of 4 equivalents of M would be interpreted as leading to the exclusive formation of M_4-MT, the addition of 5 equivalents of M would result in precisely M_5-MT, and so on up to the saturation point (where M is the metal ion of interest). While it might be considered that

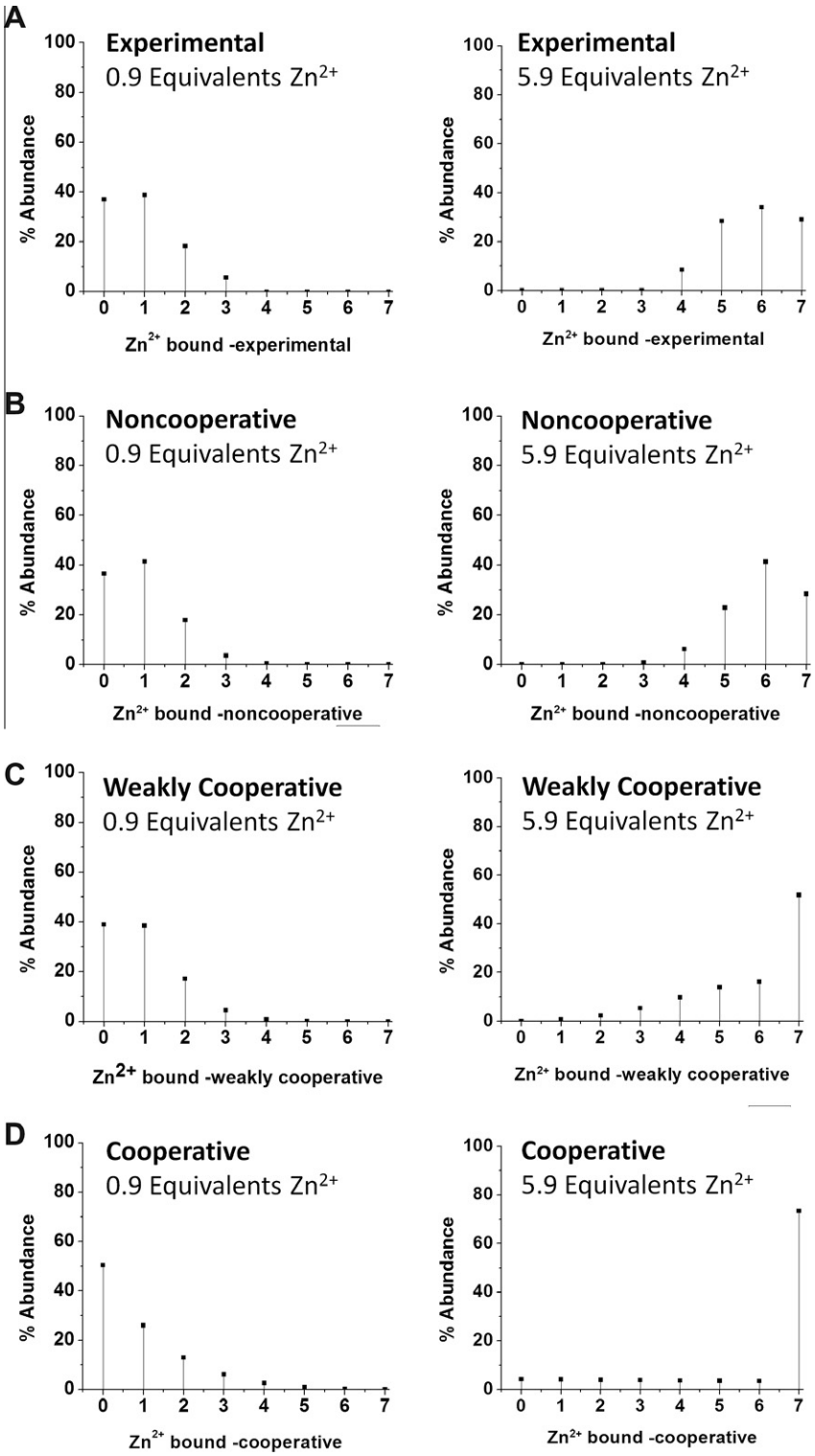

Fig. 4. ESI-mass spectral data for the metalation of apo-βα-rhMT 1a with Zn^{2+}. (A) Experimental ESI-mass spectral data for βα-rhMT 1a at the 0.9 and 5.9 equivalents-added steps of Zn^{2+}. (B) Simulated ESI-mass spectral data based upon a noncooperative mechanism. (C) Simulated ESI-mass spectral data based upon a weakly cooperative mechanism. (D) Simulated ESI-mass spectral data based upon a cooperative mechanism.

addition of 5 Zn^{2+} to H_{20}-βα-rhMT should result in formation of Zn_5-βα-rhMT this would not be the case unless the mechanism was strongly cooperative with an end point for 5 metals. As shown above, only under a strongly cooperative mechanism of metalation does the composition of MT approach homogeneity and even then slight amounts of partially metalated species are present. Under all mechanisms the metal distribution will be represented by the ratio of the relative binding constants, that is K_7:K_6:K_5:K_4:K_3:K_2:K_1. It is possible to determine the ratios of the binding affinities and consequently, the binding mechanism by calculating the expected metal distribution for each addition of metal in a stepwise titration and comparing the predicted data with the experimental data. Only ESI-mass spectral data provide the speciation at each addition of metal, allowing this comparison to be made.

Both the models and the experimental data in Figs. 3 and 4 show that in fact at every step in the titration there is a continuum of metalated species. In essence, metalation of metallothionein takes place via a number of concurrently formed species before saturation completes the fully metalated species.

Initial studies of both the metalation and demetalation reactions of MT led to hypotheses that metalation occurred in a cooperative fashion. Three important consequences of the cooperative mechanism are (1) partially metallated forms would be a very low fraction (only fully metallated and fully metal free would persist), (2) partially metallated forms would be unlikely to play a major role in cellular chemistry, and (3) oxidation of the protein would lead to complete, cooperative demetalation of the protein.

Considering recent mechanistic studies of Zn^{2+}, Cd^{2+} and As^{3+} binding to human MT [4,19] and the results presented here, it is clear that under these conditions, the mechanism of metalation is in fact noncooperative. In a noncooperative mechanism, metal binding events are independent of each other, so that: (1) significant fractions of the protein are partially metallated until saturation, and could potentially take part in cellular chemistry, and (2) partial oxidation of the protein will not necessary lead to complete demetalation of the protein. Studies of the metal binding properties of human MT-2 with Zn^{2+} have shown a series of affinities that differ by four orders of magnitude (highest affinity $K = 10^{11.8}$, lowest affinity $K = 10^{7.7}$) [25]. This range of association constants allows MT to act as a robust metallochaperone capable of accepting Zn^{2+} in cases of excess and donating Zn^{2+} in cases of deficiency. Figs. 2–4 all argue for a noncooperative mechanism of metalation, where the metal ion speciation of each protein is directly related to the number of metals added to solution.

To summarize, in this paper we have shown that ESI-mass spectral data provide key information about the mechanism of metalation of MT – specifically the metal ion speciation as a function of metals added. We have also provided the theoretical speciation for noncooperative, weakly cooperative, and strongly cooperative mechanisms. The experimental data for Zn^{2+}, Cd^{2+}, As^{3+}, and Bi^{3+} all follow a noncooperative mechanism when binding to rhMT 1a. Taken together, these results provide the framework for analyzing all MT mass spectral data in terms of the mechanism of metalation.

Acknowledgments

We thank Natural Sciences and Engineering Research Council of Canada for financial support through operating and equipment grants (M.J.S.), and the Canadian Graduate Scholarship program (D.E.K.S.). We also thank Doug Hairsine (Western Ontario) for advice on operation of the ESI mass spectrometer.

References

[1] Y. Kojima, Introduction 2 Definitions and nomenclature of metallothioneins, in: J.F. Riordan, B.L. Vallee (Eds.), Methods in Enzymology: Metallobiochemistry. Part B Metallothionein and Related Molecules, Academic Press Inc., San Diego, 1991, pp. 8–10.
[2] Y. Boulanger, I.M. Armitage, ^{113}Cd NMR study of the metal cluster structure of human liver metallothionein, J. Inorg. Biochem. 17 (1982) 147–153.
[3] T.T. Ngu, A. Easton, M.J. Stillman, Kinetic analysis of arsenic-metalation of human metallothionein: significance of the two-domain structure, J. Am. Chem. Soc. 130 (2008) 17016–17028.
[4] D.E.K. Sutherland, M.J. Stillman, The "magic numbers" of metallothionein, Metallomics 3 (2011) 444–463.
[5] B.A. Messerle, A. Schaffer, M. Vasak, J.H.R. Kagi, K. Wuthrich, Three-dimensional structure of human [$^{113}Cd_7$] metallothionein-2 in solution determined by nuclear magnetic resonance spectroscopy, J. Mol. Biol. 214 (1990) 765–779.
[6] B.A. Messerle, A. Schaffer, M. Vasak, J.H.R. Kagi, K. Wuthrich, Comparison of the solution conformations of human [Zn_7]-metallothionein-2 and [Cd_7]-metallothionein-2 using nuclear magnetic resonance spectroscopy, J. Mol. Biol. 225 (1992) 433–443.
[7] M.J. Stillman, Metallothioneins, Coord. Chem. Rev. 144 (1995) 461–511.
[8] M. Good, R. Hollenstein, P.J. Sadler, M. Vasak, ^{113}Cd NMR studies on metal-thiolate cluster formation in rabbit Cd(II)-metallothionein: evidence for a pH dependence, Biochemistry 27 (1988) 7163–7166.
[9] P.M. Gehrig, C. You, R. Dallinger, C. Gruber, M. Brouwer, J.H.R. Kagi, P.E. Hunziker, Electrospray ionization mass spectrometry of zinc, cadmium, and copper metallothioneins: evidence for metal-binding cooperativity, Protein Sci. 9 (2000) 395–402.
[10] D.E.K. Sutherland, M.J. Stillman, Noncooperative cadmium(II) binding to human metallothionein 1a, Biochem. Biophys. Res. Commun. 372 (2008) 840–844.
[11] P. Palumaa, E. Eriste, O. Njunkova, L. Pokras, H. Jornvall, R. Sillard, Brain-specific metallothionein-3 has a higher metal-binding capacity than ubiquitous metallothioneins and binds metals noncooperatively, Biochemistry 41 (2002) 6158–6163.
[12] T.T. Ngu, M.J. Stillman, Arsenic binding to human metallothionein, J. Am. Chem. Soc. 128 (2006) 12473–12483.
[13] T.T. Ngu, J.A. Lee, M.K. Rushton, M.J. Stillman, Arsenic metalation of Seaweed *Fucus vesiculosus* metallothionein: the importance of the interdomain linker in metallothionein, Biochemistry 48 (2009) 8806–8816.
[14] T.T. Ngu, S. Krecisz, M.J. Stillman, Bismuth binding studies to the human metallothionien using electrospray mass spectrometry, Biochem. Biophys. Res. Commun. 396 (2010) 206–212.
[15] T.T. Ngu, J.A. Lee, T.B.J. Pinter, M.J. Stillman, Arsenic-metalation of triple-domain human metallothioneins: support for the evolutionary advantage and interdomain metalation of multiple-metal-binding domains, J. Inorg. Biochem. 104 (2010) 232–244.
[16] T.T. Ngu, M.D.M. Dryden, M.J. Stillman, Arsenic transfer between metallothionein proteins at physiological pH, Biochem. Biophys. Res. Commun. 401 (2010) 69–74.
[17] J. Chan, Z. Huang, I. Watt, P. Kille, M.J. Stillman, Characterization of the conformational changes in recombinant human metallothioneins using ESI-MS and molecular modeling, Can. J. Chem. 85 (2007) 898–912.
[18] D.E.K. Sutherland, M.J. Willans, M.J. Stillman, Single domain metallothioneins: Supermetlation of human MT 1a, J. Am. Chem. Soc. 134 (2012) 3290–3299.
[19] D.E.K. Sutherland, K.L. Summers, M.J. Stillman, Noncooperative metalation of metallothionein 1a and its isolated domains with zinc, Biochemistry, doi: 10.1021/bi3004523.
[20] K.E. Rigby-Duncan, M.J. Stillman, Evidence for noncooperative metal binding to the α domain of human metallothionein, FEBS J. 274 (2007) 2253–2261.
[21] D.E.K. Sutherland, M.J. Willans, M.J. Stillman, Supermetalation of the β domain of human metallothionein 1a, Biochemistry 49 (2010) 3593–3601.
[22] G. Meloni, T. Polanski, O. Braun, M. Vasak, Effects of Zn^{2+}, Ca^{2+}, and Mg^{2+} on the structure of Zn_7 metallothionein-3: Evidence for an additional zinc binding site, Biochemistry 48 (2009) 5700–5707.
[23] N. Felitsyn, M. Peschke, P. Kebarle, Origin and number of charges observed on multiply-protonated native proteins produced by ESI, Int. J. Mass Spectrom. 219 (2002) 39–62.
[24] P. Kebarle, U.H. Verkerk, Electrospray: From ions in solution to ions in the gas phase, what we know now, Mass Spectrom. Rev. 28 (2009) 898–917.
[25] A. Krezel, W. Maret, Dual nanomolar and picomolar Zn(II) binding properties of metallothionein, J. Am. Chem. Soc. 129 (2007) 10911–10921.